RF thermal and new cold part design studies on a TTF-III input coupler for Project-X

PEI Shi-Lun(裴士伦)[1;1)]   Chris E Adolphsen[2]   LI Zeng-Hai(李增海)[2]

Nikolay A Solyak[3]   Ivan V Gonin[3]

[1] Institute of High Energy Physics, Chinese Academy of Sciences, Beijing 100049, China
[2] SLAC National Accelerator Laboratory, Menlo Park, California 94025, USA
[3] Fermi National Accelerator Laboratory, Batavia 60510, Illinois, USA

Abstract: An RF power coupler is one of the key components in a superconducting (SC) linac. It provides RF power to the SC cavity and interconnects different temperature layers (1.8 K, 4.2 K, 70 K and 300 K). The TTF-III coupler is one of the most promising candidates for the High Energy (HE) linac of Project X, but it cannot meet the average power requirements because of the relatively high temperature rise on the warm inner conductor, so some design modifications will be required. In this paper, we describe our simulation studies on the copper coating thickness on the warm inner conductor with RRR values of 10 and 100. Our purpose is to rebalance the dynamic and static loads, and finally lower the temperature rise along the warm inner conductor. In addition, to get stronger coupling, better power handling and less multipacting probability, one new cold part design was proposed using a 60 mm coaxial line; the corresponding multipacting simulation studies have also been investigated.

Key words: RF thermal effect, TTF-III input coupler, multipacting, dynamic RF power loss, static thermal loss

PACS: 41.20.Jb, 44.05.+e, 44.10.+I   **DOI:** 10.1088/1674-1137/36/2/013

1 Introduction

Project X is a high intensity proton facility conceived to support a world-leading program in neutrino and flavor physics over the next two decades at Fermilab. The RF coupler requirements for the HE linac are depicted in Table 1 [1]. For safety margin consideration, the coupler should be able to handle ∼2.2 MW (∼10% overhead) peak power during the ∼0.2 ms filling time and ∼550 kW (∼10% overhead) during the ∼1.25–2.5 ms flat top with a total average power of ∼15 kW [2].

TTF-III coupler is one of the most promising candidates for the HE linac since it is a proven component of the European XFEL design. It has been demonstrated that a TTF-III coupler can handle ∼2 MW peak power and up to 10 kW of average power with an air cooled central conductor [3]. However, the TTF-III coupler may meet the peak power

Table 1.   RF coupler requirements for the HE linac.

parameters	1 MW	2 MW upgrade	4 MW upgrade
beam energy /GeV	8	8	8
current/mA	20	20	20
repetition rate/Hz	5	10	10
gradient (β=1)/MV/m	25	25	25
$Q_{ext}/10^6$	1.25	1.25	1.25
filling time/ms	0.212	0.212	0.212
T_{pulse} (flat-top)/ms	1.25	1.25	2.5
T_{total}/ms	1.465	1.465	2.712
P_{peak} (coupler)/kW	500	500	500
$P_{average}$ (coupler)/kW	3.7	7.3	13.6

requirements for all Project X operating scenarios, but cannot meet the average power requirements because of the relatively high temperature rise on the warm side inner conductor, which might result in

melting or desquamating of the cooper coating. Some design modifications will be required; one simple way is to increase the copper coating thickness on the warm inner conductor.

It has been known that for dynamic RF power losses a higher copper RRR is better, but for static thermal losses a lower RRR is better. In order to rebalance the dynamic and static loads, the best compromise for the RRR value of the copper coating should be found by studying the RF-thermal effect at different copper RRR values. For the TTF-Ⅲ coupler, the RRR upper limit was set at 80 to satisfy the requirement of maximum thermal power transmitted at the 4 K shield of 0.5 W by every coupler[1].

Here for TTF-Ⅲ like coupler applied to Project X, we studied RF-thermal effects with a different copper coating thickness on the warm inner conductor when the copper RRR values are 10 and 100 respectively. In addition, to facilitate the multipacting problem [2] and get better power handling capability, one new cold part design using a 60 mm coaxial line was proposed.

2 TTF-Ⅲ coupler

Figure 1 shows the TTF-Ⅲ RF input power coupler design [4, 5]. It has 4 fixed temperature layers: an outside connection layer to a 300 K room temperature environment, 70 K and 4.2 K shield connection layers to cryogenics, and the SC cavity flange at the 1.8 K temperature layer. Except for the coupler cold part antenna, which is made of pure copper, the other inner and outer conductors are made of stainless steel but are coated with copper. The TTF-Ⅲ coupler has 2 ceramic windows (warm and cold) and 3 bellows. A standard TTF-Ⅲ coupler configuration has a 10 μm copper coating on both the cold and warm outer conductors, but a 30 μm coating on the on warm inner conductor.
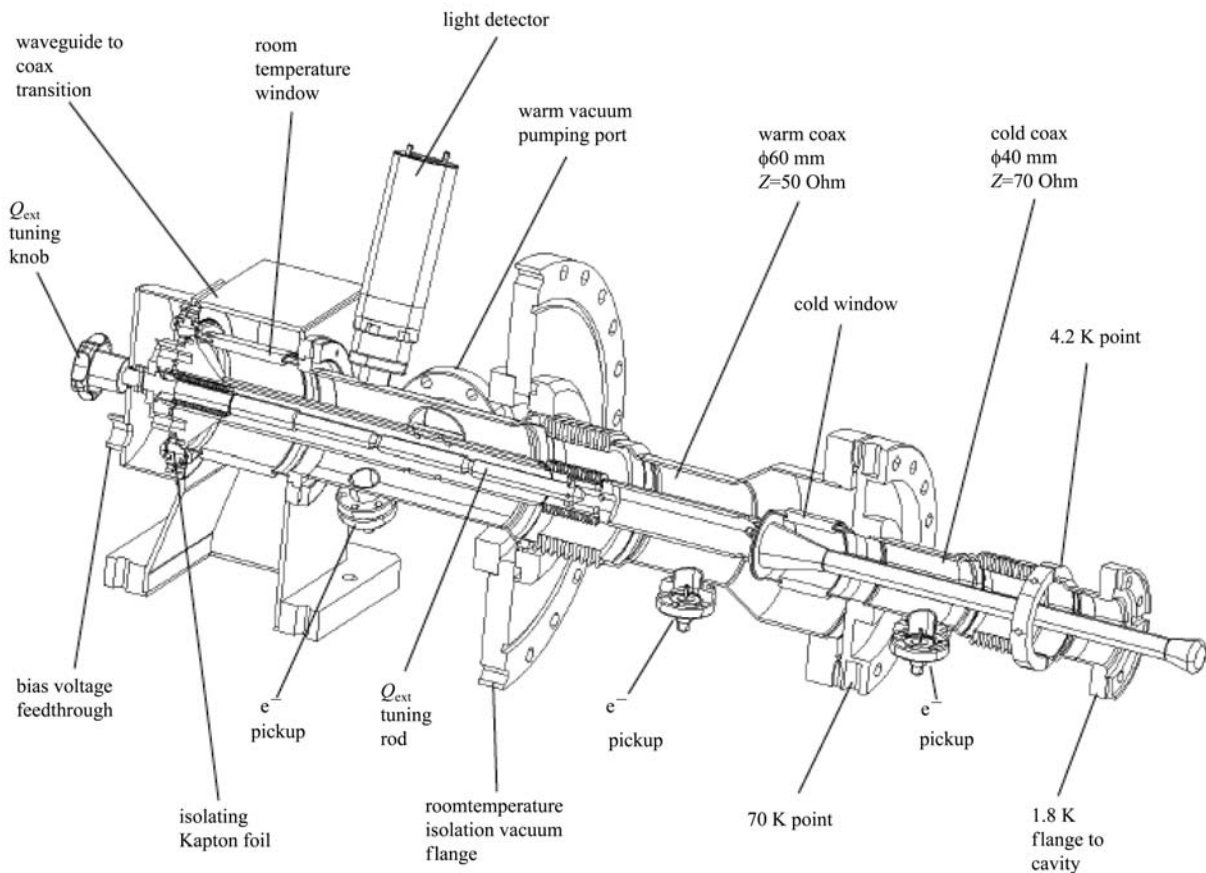

Fig. 1. TTF-Ⅲ RF input power coupler design.

1) Moeller W, Prat S, Haase A et al. Private Communication

3   ANSYS simulations

With the High Frequency and Steady State Thermal solver modules in the multi-physics software package ANSYS [6], numerical RF-thermal coupled finite element analysis (FEA) has been carried out. Currently the ANSYS High Frequency module has the limitation that only 3D elements can be used. To minimize CPU time and memory usage, one axis-symmetric 3D model with a 1° azimuth angle was created to perform the analysis. By using one program for all the simulations any problems of transferring loads were eliminated.

A complete analysis cycle required 5 steps as outlined below. Due to the temperature dependence of material properties shown in Figs. 2 and 3 [5], Step 5 needs to be iterated several times to get a stable thermal solution until the error between two consecutive iterations reaches the specified value. The simulation result in Step 4 serves as the initial condition.

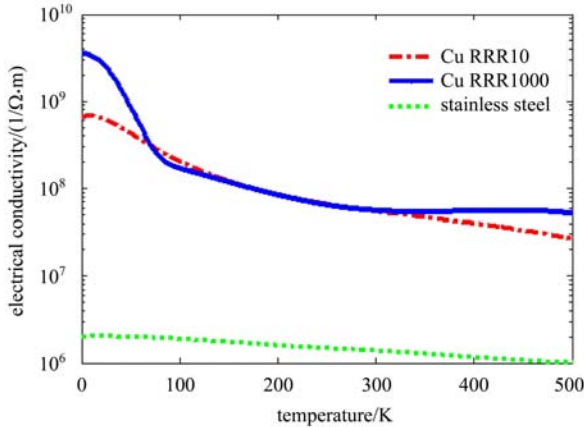1) The vacuum volume and the copper coating

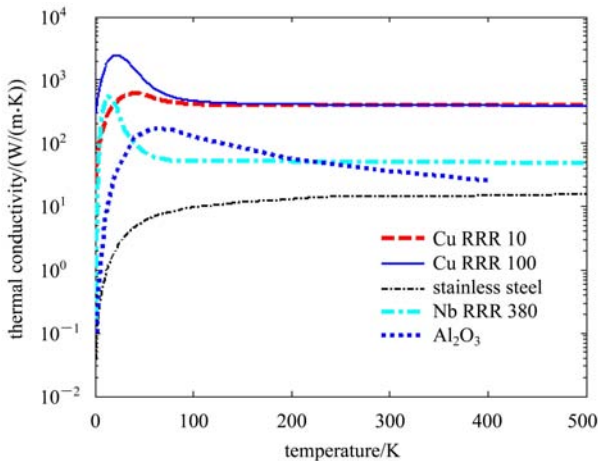Fig. 2.   Electrical conductivities for different temperatures.

Fig. 3.   Thermal conductivities for different temperatures.

volume were meshed with a common surface interface mesh. The analysis domain volumes were defined with APDL (ANSYS Parametric Design Language) macro language [6]. The common surface mesh created at this step is the key for ease of transfer of the RF wall losses onto the thermal model.

2) The copper coating volume and the rest metallic volumes were meshed with SOLID90 20-Node thermal solid element, but assigned with different materials. The pure copper antenna was also modeled with two separate volumes: copper coating and copper metallic volumes.

3) With a HF120 high frequency brick solid element, harmonic analysis was performed in the vacuum volume and the cold ceramic window volume for specified average input power. The impedance boundary condition of copper at room temperature (300 K) was applied to the common surface. Using the built-in macro 'SPARM' and 'HFPOWER', it is possible to calculate the scattering (S) parameters and the total time averaged dielectric losses.

4) By using built-in macro 'ETCHG', the HF120 brick element was converted to a SOLID90 thermal element. The RF wall losses and the ceramic power losses obtained in Step 3 were applied as thermal heat flux surface loads and heat generation body loads respectively. With the 4 fixed temperature layers (1.8 K, 4.2 K, 70 K and 300 K) as external temperature boundary conditions, the 'static + dynamic' temperature profile in the metallic volume can be calculated. For the 'static' case, the heat flux surface loads and the heat generation body loads were ignored.

5) With the temperature profile obtained from Step 4 or the previous iteration, new thermal flux surface loads on each of the common surface elements can be recalculated using a simple scaling relation ($P \sim \sigma(T)^{-1}$, P is the RF power loss, while σ is the electrical conductivity, which is a function of temperature T) and reapplied in the following iterating thermal calculation.

The temperature profile along inner and outer conductors has been calculated for different copper coating thicknesses on the warm inner conductor with RRR=10 and 100, supposing the coupler to be operating in a continuous regime with a 15 kW average input power at the 1.3 GHz design frequency.

4   Simulation results

4.1   RF power losses

Figure 4 shows one typical RF wall loss distribu-

tion for stable travelling wave operation. Here 100 μm and 10 μm RRR=100 copper were coated on the warm inner and all outer conductors respectively, and the temperature dependence of the material properties was also considered. The bellow parts can be clearly identified from the plot.
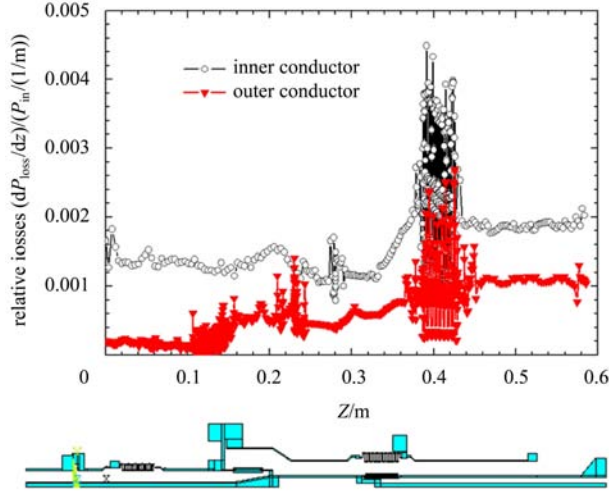

Fig. 4. Typical RF wall loss distribution for the TW case.

Both S3P [7] and ANSYS were used to calculate the power losses in the 70 K ceramic window with $\varepsilon=9$ and $tg\delta = 10^{-4}$. Fig. 5 shows the electric and magnetic field distribution inside the vacuum and ceramic window volumes. Different from the power loss ratio ($P_{\mathrm{loss,win}}/P_{\mathrm{in}}$) calculation results 1.94×10^{-4} in Ref. [5], the ratio here is around 1.23×10^{-4} for both FEM codes, similar results were obtained for a finer mesh.
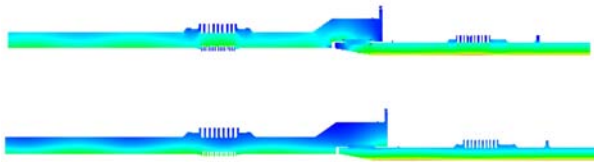

Fig. 5. Electric (upper) and magnetic (lower) field distribution inside the coupler.

4.2 Thermal calculation results

Figures 6 and 7 show the temperature distribution along the inner conductor of the TTF-III coupler for RRR=10 and RRR=100. The copper coating on the outer conductor was fixed at 10 μm. With an increasing copper RRR value and coating thickness, the maximum temperature rise on the warm inner conductor decreases.

Corresponding to Fig. 6, Fig. 8 shows the temperature distribution along the outer conductor for

RRR=10. It can be clearly seen that increasing the copper coating thickness on the warm inner conductor has no big effect on the outer conductor temperature profile. Similar results can be obtained for RRR=100.
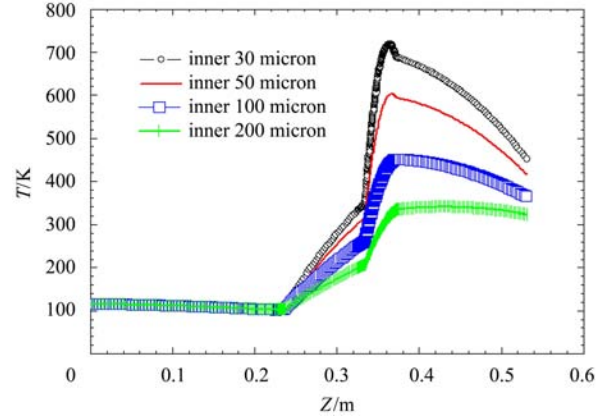

Fig. 6. Inner conductor temperature distribution with a 10 μm RRR=10 copper coating on the outer conductor.
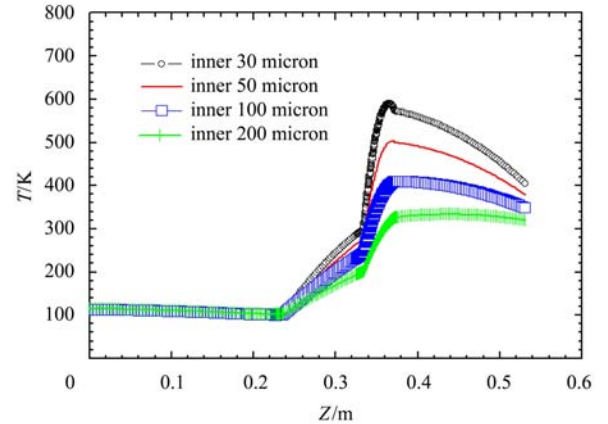

Fig. 7. Inner conductor temperature distribution with 10 μm RRR=100 copper coating on outer conductor.
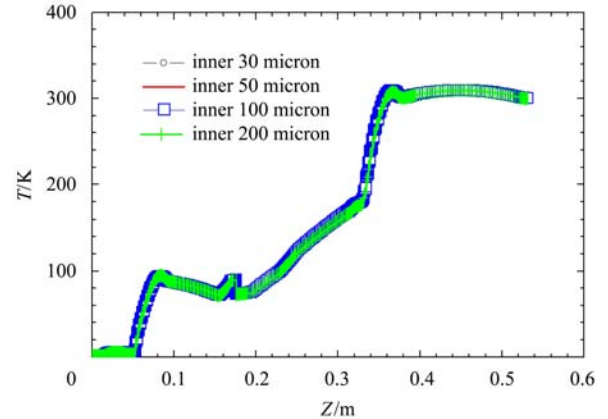

Fig. 8. Outer conductor temperature distribution with a 10 μm RRR=10 copper coating on the outer conductor.

Figures 9 and 10 show the typical temperature distributions for 'static' and 'static + dynamic' cases. 100 μm and 10 μm copper (RRR=100) was coated on the inner and outer conductors respectively.
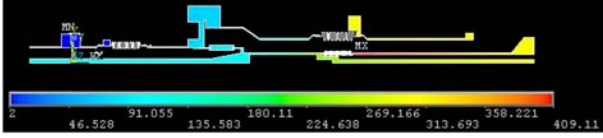

Fig. 9.   Typical temperature distribution for 'static' case.

Table 2 shows all the obtained cryogenic power loss data and the maximum temperature rise on the

warm inner conductor. With the increasing copper coating thickness from 30 μm to 200 μm, the static cryogenic loss increased from 2.785 W to 5.351 W for RRR=10 and from 2.859 W to 5.580 W for RRR=100, the dynamic cryogenic loss decreased 8% for RRR=10 and 1% for RRR=100.
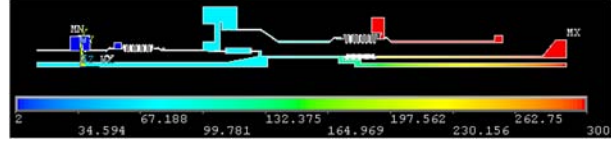

Fig. 10.   Typical temperature distribution for 'static+dynamic' case.

Table 2.   Power losses at different temperature layers and the maximum temperature on the warm inner conductor (the copper coating on the outer conductor was fixed at 10 μm).

Inner Coating	RRR	case	P(2 K)/W	P(4 K)/W	P_{in}(70 K)/W	P_{out}(70 K)/W	P_{win}(70 K)/W	P_{total}/W	T_{max}/K
30	10	static	0.008	0.240	1.454	1.083	0	2.785	718
30		dynamic	0.357	0.790	13.45	4.574	1.84	21.01	
50		static	0.008	0.240	1.804	1.083	0	3.135	603
50		dynamic	0.356	0.793	13.53	4.527	1.85	21.06	
100		static	0.008	0.241	2.609	1.082	0	3.940	450
100		dynamic	0.356	0.787	12.99	4.592	1.89	20.61	
200		static	0.008	0.241	4.021	1.081	0	5.351	340
200		dynamic	0.361	0.792	11.86	4.515	1.81	19.34	
30	100	static	0.049	0.614	1.493	0.703	0	2.859	590
30		dynamic	0.251	0.381	12.23	4.316	1.84	19.02	
50		static	0.049	0.614	1.865	0.702	0	3.230	503
50		dynamic	0.251	0.381	12.36	4.270	1.85	19.12	
100		static	0.049	0.614	2.719	0.702	0	4.084	409
100		dynamic	0.251	0.381	12.55	4.341	1.89	19.41	
200		static	0.049	0.615	4.215	0.701	0	5.580	333
200		dynamic	0.255	0.385	12.08	4.266	1.814	18.804	

5   New cold part design

For coax geometries, the power level for the occurrence of multipacting scales with the 4th power of the diameter of the outer conductor [8]. The multipacting power bands can be increased significantly by using a cold part design with a larger diameter. It has been shown the TTF-III coupler has a tendency to have a long initial high power processing time, which might be caused by multipacting [9]. One new cold part using a 60 mm coaxial line was designed, which has a relatively longer taper in the pure copper antenna region.

Figure 11 shows the electric field profile for stable travelling wave operation. Multipacting was simulated with particle tracking code Track3P [7]. Fig. 12 shows the multipacting simulation result. Compared with the results in Ref. [9], the multipacting impact energy has been greatly reduced up to a 4 MW input power level, indicating that the new design will have
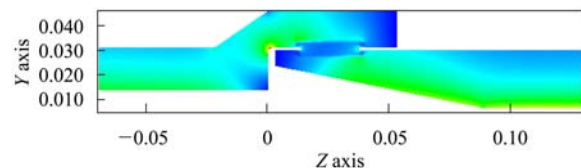

Fig. 11.   Electric field profile for the new cold part design.

impact energy vs multipacting particles location z
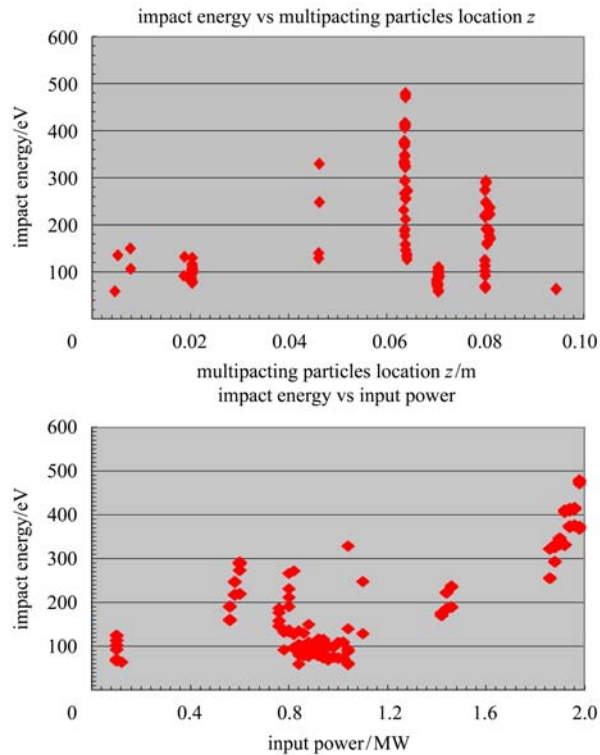

impact energy vs input power

Fig. 12.   Multipacting impact energy as a function of axial position (upper) and input RF power level (lower).

better power handling capability and less multipacting probability.

6   Conclusions

RF-thermal calculations on the TTF-Ⅲ input coupler for a copper coating ranging from 30 μm to 200 μm (RRR=10 and 100) on the warm inner conductor have been done. It shows that the dynamic load is not always constant because of the complicated nonlinear temperature dependence of electric and thermal conductivities. If the tolerable temperature rise is ∼ 150°, a copper coating thickness of ∼100 μm would be enough. Increasing the copper RRR value does help to reduce the maximum temperature rise. To further decrease the temperature rise on the warm inner conductor, an air cooled center conductor would help significantly [10].

One new cold coupler part using a 60 mm coaxial line was designed. From Track3P simulation studies, the new design has less multipacting probabilities than the old design. The disadvantage of the new design is that the field asymmetry near the antenna region is more severe, which might result in bigger RF kick and wakes, and needs to be studied further.

References

1 Project X Research Design & Development Plan. Version 2.2, 2009. 3

2 Solyak N. Power Couplers for ILC and Project X. DOE SRF Review, 2009. 5

3 Solyak N, Yakovlev V. Project X Coupler Requirements. Project X Collaboration Meeting, FNAL, 2008. 11

4 Moeller W. High Power Coupler for the TESLA Test Facility. Proc. of the 9th Workshop on RF Superconductivity. Santa Fe, USA, 1999. 577–581

5 Dohlus M, Kostin D, Moeller W. TESLA RF Power Coupler Thermal Calculations. Proc. of LINAC 2004. Lubeck, Germany, 2004. 174–176

6 ANSYS is a trademark of SAS Inc., (www.ansys.com)

7 Li Z, Akcelik V, Candel A et al. Towards Simulation of Electromagnetics and Beam Physics at the Petascale. Proc. of PAC07. Albuquerque, New Mexico, USA, 2007. 889–893

8 Somersalo E, Yla-Oijala P. Analysis of Multipacting in Coaxial Lines. Proc. of PAC95. Dallas, Texas, USA, 1995. 1500–1502

9 Ge L, Adolphsen C, Ko K et al. Multipacting Simulations of TTF-Ⅲ Power Coupler Components. Proc. of PAC07. Albuquerque, New Mexico, USA, 2007. 2436–2438

10 Veshcherevich V, Belomestnykn S, Quigley P et al. High Power Tests of Input Couplers for Cornell ERL Injector. Proc. of SRF Workshop 2007. Beijing, China, 2007. 517–519